Suárez, M.; Fernández, A.; Díaz, L.; Sobrados, I.; Sanz, J.; Borrell Tomás, MA.; Palomares, F.... (2020). Synthesis and sintering at low temperature of a new nanostructured beta-Eucryptite dense compact by spark plasma sintering. Ceramics International. 46(11):18469-18477. https://doi.org/10.1016/j.ceramint.2020.04.152

Spark plasma sintering of kaolin and lithium carbonate mixtures. Formation of a new nanostructured Li-geopolymer ceramics.

M. Suárez[1], A. Fernández[1], L. A. Díaz[1], I. Sobrados[2], J. Sanz[2], A. Borrell[3], F. J. Palomares[2], R. Torrecillas[1], J.S. Moya[2].

[1]Nanomaterials and Nanotechnology Research Center (CINN-CSIC), Universidad de Oviedo (UO), Principado de Asturias (PA), Avda. de la Vega 4-6, 33940 El Entrego, Spain

[2]Instituto Ciencia de Materiales de Madrid, CSIC. 28049 Madrid, Spain.

[3]Instituto de Tecnología de Materiales, Universitat Politècnica de València, Camino de Vera s/n, 46022, Valencia, Spain

Abstract

The solid state reaction between kaolin and Li_2CO_3 with a 1:1 molar composition has been studied in the temperature range 380ºC-550ºC. The role played by Li_2CO_3 (basic medium) in the thermal transformation of the kaolin has been investigated by X-Ray diffraction, SEM, TEM, MAS-NMR and XPS techniques. For the first time, a nanostructured high density β-eucryptite (<10nm) has been obtained by SPS at 550ºC in high vacuum. The atmosphere used in sintering treatments has a determinant role in lithium migration and crystallization of β-eucryptite. In the case of low vacuum treatments, an amorphous $LiAlSiO_4$ geopolymer was obtained. Due to exclusive properties and performances of β-eucryptite based materials, the results reported in the present investigation open new perspectives for new nanostructured and amorphous functional materials with null thermal expansion, ionic conduction and remarkable mechanical properties.

Keywords: kaolin, geopolymer, β-eucryptite, Spark plasma sintering

1. Introduction

The term geopolymer was first used by Davidovits in the 1970´s for alumina-silicate polymers formed in alkaline environment [1]. They are considered as alkali-activated binders composed by (3D) three-dimensional Si-O-Al frameworks. The chemical composition of amorphous geopolymers is similar to the zeolites, but polymerized tetrahedral networks formed display remarkable properties: thermal and chemical stability, high compressive strength, low creep, good acid resistance and low shrinkage [2].

Geopolymers are usually produced by the reaction of aluminosilicates with an alkaline activator that contains alkali hydroxide, silicates, aluminates, carbonates or sulphates or a combination thereof [3]. These materials cure and harden at ambient temperature. Physical, mechanical, chemical and thermal properties of the geopolymers depend on the microstructure derived from raw material used in processing conditions. In particular, different sources of aluminosilicates can be used: natural reactive aluminosilicate powders (e.g. diatoms, non-thermally activated clays, etc..), activated aluminosilicates such as metakaoline or by-products supplied by other industrial processes (e. g. fly ash, low calcium slags and mining waste) [4,5,6,7]. Pure metakaoline obtained by thermal activation of kaolinite provides high reactivity [8], compressive and flexural strengths [9], resistance to acid attack and durability to geopolymer formed.

Besides a reactive aluminosilicate source, an alkaline activator is also required to produce a geopolymer. It is well known that the type of cation involved in the activation reaction affects the microstructure development of the geopolymers. The alkaline metal cation balances the negative framework charge associated with Al tetrahedral of tetrahedral networks, being Na^+ and K^+ the most common alkali metal cations used in the geopolymer reaction [10,11,12,13].Most of the studies reported in the literature of geopolymers have focused mainly on the reaction between metakaoline and NaOH or KOH [14], few studies have been carried out with incorporation of lithium.

The reaction between the kaolin and the lithium carbonate to give β-eucryptite was reported previously by A. Garcia-Verduch and J. S. Moya in a pioneering/preliminary work [15]. These authors established that the initial reaction between both reactants proceeds through a mechanism of Li^+ and H^+ counter-diffusion. Subsequently, R. Torrecillas et al [16,17,18,19] reported low or null thermal expansion materials from mixtures of kaolin and Li_2CO_3 followed by sintering in conventional or spark plasma sintering at temperatures between 1100 and 1400ºC. A. Borrell et al [20] compare the influence of the sintering methodology into the properties of lithium aluminosilicate materials; however, to date there are no works reporting thermal evolution of intermediate amorphous polymerized structures (geopolymers) that are formed in the early stages of the reaction between kaolin and lithium carbonate.

Geopolymers have already find applications in different fields of industry related to the automotive and aerospace industries, non-ferrous foundries and metallurgy, civil engineering, cements and concretes, ceramics and plastics industries, waste management, art and decoration, retrofit of buildings, thermal insulation, etc [1,7]. The geopolymer manufacturing, unlike Portland cement, no consume energy, making that geopolymers become a potential alternative binder to ordinary Portland cement (OPC) in some applications, lowering significantly emission of greenhouse gases. According to the literature, it is

estimated that for every kilogram of OPC manufactured, 0.66-0.82 Kg of CO_2 are emitted into the atmosphere [21], making geopolymers to be considered as environmental friendliness binders. Taking into account the possible Li ion conductivity, application of Li-geopolymers could be extended to thermal batteries, solid electrodes, electrothermal devices, etc. [22,23]. The elimination of grain boundary between particles should improve overall conductivity of thick films electrolytes.

The aim of this work is to investigate the low temperature (380ºC-550ºC) reactions between kaolin and Li_2CO_3 under different atmospheres (air, low and high vacuum) and materials produced by conventional and Spark Plasma (SPS) sintering. Li-geopolymers formed at intermediate treatments will be characterized by X-ray Diffraction, Scanning Electron Microscopy, Transmission Electron Microscopy techniques. On the other hand, cation coordination and tetrahedral networks formed at increasing temperatures will be analyzed with X-ray Photoelectron Spectroscopy and solid-state MAS-Nuclear Magnetic Resonance spectroscopies.

2. Materials and methods

2.1. Starting materials

In this study, a highly pure kaolin from Lage, La Coruña, Spain, with a chemical composition (wt%): SiO_2, 45.00; Al_2O_3, 38.20; Fe_2O_3, 0.08; CaO, 0.21; MgO, 0.01; Na_2O, 0.01; K_2O, 0.41; loi, 16.26, with an average particle size in volume of d_{50}= 1.13µm and a BET specific surface area of 20.32 m^2/g was used as starting material. The lithium carbonate Li_2CO_3 (Sigma-Aldrich) was used as alkaline activator.

2.2. Powder processing and sintering

Prior alkaline activation, the kaolin was sieved through <63µm mesh. Then, kaolin: Li_2CO_3 (1:1 molar ratio) mixtures were prepared by mixing powder in propanol liquid media using a ball mill for 24 hours. The homogeneous mixture was dried at 100ºC during 24h and treated at 380ºC, 470ºC and 550ºC for different times in air atmosphere. In each thermal treatment, the starting kaolin was used as reference.

Kaolin: Li_2CO_3 (1:1 molar ratio) mixtures, heated in air at 550ºC for 30min, were grounded and sieved through <63 microns mesh and sintered under different atmospheres: in air (after uniaxial pressing in a conventional furnace) or in low and high vacuum in a Spark Plasma Sintering (SPS) apparatus (FCT-HP D 25/1). In this case, powders were first placed into a graphite die (20mm inner diameter), applying an uniaxial pressing of 80MPa and then sintered five minutes at 500 and 550ºC using a heating rate of 50ºC/min and a vacuum of 3 and 0.3mbar for low and high vacuum experiments. Sintered samples were grounded and sieved again through <63 microns mesh for further characterization.

2.3. Characterization techniques

X-ray diffraction (XRD) patterns of kaolin, kaolin: Li_2CO_3 (1:1 molar ratio) mixtures and sintered samples were collected on a Bruker Advanced Powder X-ray diffractometer by using Cu-Kα radiation (λ= 0.15406nm) in the range from 5º to 70º. The step size was 0.02˚ and the step time 0.5s. The identification of the crystalline phases was realized by using diffraction pattern files provided by JCPDS (International

Centre for Diffraction Data).To study the alkaline activation, kaolin and kaolin: Li_2CO_3 (1:1 molar ratio) mixtures, treated at different temperatures and times in air, were mixed homogeneously with the α-alumina standard. The mixture was dried and sieved before X-ray diffraction characterization.

^{27}Al, ^{29}Si, and ^{7}Li MAS-NMR spectra of powder samples were recorded at 104.4, 79.8 and 155.5MHz, with the MAS technique (spinning the samples around an axes inclines 54º47´with respect the external magnetic field) in a Bruker AVANCE 400 spectrometer. The spinning frequency was in the range of 10-20 kHz. To avoid saturation effects, spectra were recorded after π/2 and π/8 (4 and 2μs) pulses in Si (or Li) and Al signals. Measurements were carried out at room temperature with TMS, $AlCl_3$ and LiCl 1M solutions as external standards.

X-ray photoelectron spectroscopy (XPS) was used to characterize the surface chemistry of the samples. XPS spectra were acquired in an UHV chamber under a base pressure of 10^{-10}mbar, equipped with a hemispherical electron energy analyzer (SPECS Phoibos 150 spectrometer) and a 2D delay-line detector (2D-DLD), using the Mg-Kα (1253.6eV) as x-ray source, operating at 200W. XPS spectra were recorded at the normal emission take-off angle. Survey detailed core level scans data were recorded with 20eV pass energy and 0.5 and 0.05eV steps, respectively. To correct surface charging effects, absolute binding energies of XPS spectra were referred to C1s peak at 284.5eV. Data processing was performed using CasaXPS software (Casa Software Ltd., Cheshire, UK).

The microstructural characterization of kaolin raw material powder and sintered samples was performed by field emission scanning electron microscopy (FESEM) on a Quanta FEG 650 in the secondary electron mode. For FESEM characterization, fracture surface, polished surface and 10 seconds (1%HF + 1%HNO_3) immersed etched surface were examined. The surface was coated with an electro-conductive iridium film for good conductivity by the sputtering method.

The apparent density of the studied samples was determined by using the Archimedes principle. Previously, 30 minutes vacuum treatment was used to remove the air inside of pores. Then the penetration of water inside the pores of the sample was forced. After this, the apparent porosity was calculated using the equation 1.

$$\rho(\%) = \frac{w_1}{w_2 - w_3}\,100 \qquad \text{Eq. 1}$$

Where w_1 is the mass of the dried sample, w_2 is the mass of the saturated sample weighed in air, and w_3 is the apparent mass of the saturated sample weighed in liquid.

The TEM lamellas were produced by standard ion beam-scanning electron microscopy lift-out procedures, using a Zeiss Auriga Compact system. They were shaped and thinned with a 30kV Ga ion beam and then polished on both sides with 5kV and 2kV beams to remove amorphous surface phases. The lamellas were then analyzed in bright field by high-resolution transmission electron microscopy (HRTEM) mode on a JEOL JEM 2100F with an acceleration voltage of 200kV with a field emission gun.

3. Results and discussion

Kaolinite, $Al_2Si_2O_5(OH)_4$, structure is formed by Si tetrahedral layers that share oxygen with Al octahedral layers [24]. Under normal environmental conditions, kaolin is stable but thermal treatments above 400ºC produces the dihydroxylation of kaolinite, giving the metakaolin ($Al_2Si_2O_7$) as intermediate phase [25]. The microstructure of kaolinite raw material is shown in Fig.1. It can be seen that kaolinite crystals consist on roughly hexagonal and plate-like structures ranging from 0.5 to 1 micron in size.

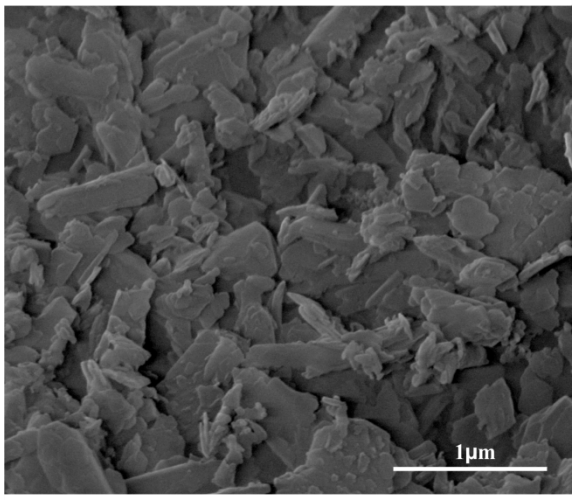

Figure 1. FESEM image of kaolinite raw material powder

In this work, kaolin and kaolin: Li_2CO_3 (1:1 molar ratio) homogeneous mixtures were subjected to different thermal treatments listed in Table 1. The heating rate used in treatments was 5ºC/min. Solid state reactions take place between kaolin and lithium carbonate (380ºC-550ºC) since the first appearance of liquid phase only takes place at the melting point of lithium carbonate (618ºC).

Calcination temperature (ºC)	Time(h)
380	0/ 5/ 20/ 40/ 70/ 100
470	1/ 2/ 6/ 16
550	0.5/ 1/ 2

Table 1: Thermal treatment in air and time of calcination for kaolin and kaolin: Li_2CO_3 (1:1 molar ratio)

3.1. X-ray diffraction

XRD patterns of kaolin and kaolin: Li_2CO_3 (1:1 molar ratio) materials are shown in Fig. 2, for different temperatures and times of calcination. The X-ray pattern of kaolin raw material shows a high degree of crystallinity as illustrated in SEM microstructures. According to depicted patterns (Fig. 2a), kaolinite is the only mineralogical phase present. In case of kaolin: Li_2CO_3 (1:1 molar ratio) material (Fig. 2b), additional 30.5°, 31.8°, 34.1° and 36.9° peaks of Li_2CO_3 were observed. The intensity of the kaolinite peaks slightly decrease with temperature and times of calcination, being more evident after 100h at 380ºC when kaolin starts to dehydroxylate. At 380ºC the dehydroxylation is a reversible process [25] but when long treatment times are used the structure of the kaolinite collapses.

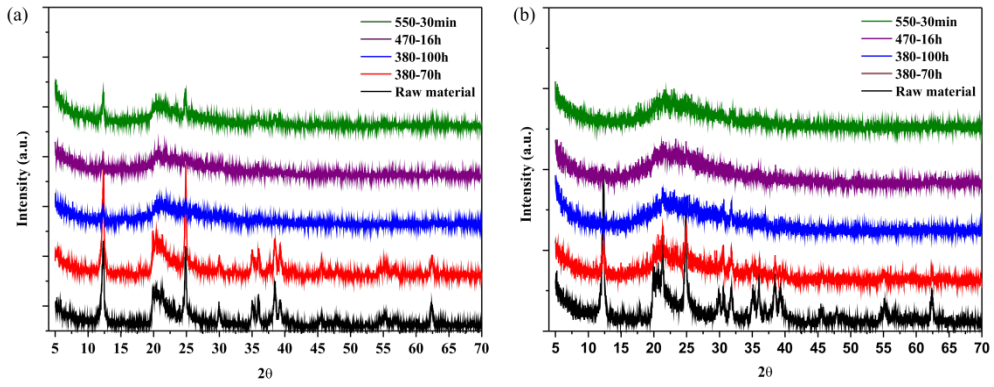

Figure 2. XRD patterns of kaolin (a) and kaolin: Li_2CO_3 (1:1 molar ratio) (b) raw material (black line) and treated at 380ºC/70h (red line), 380ºC/100h (blue line), 470ºC/16h (purple line) and 550ºC/30 minutes (green line) in air.

The transformation of kaolin into metakaolin starts somewhere between 400ºC and 500ºC, producing a gradual variation of the interlayer distances as thermal treatments progress [24]. In case of kaolin: Li_2CO_3 (1:1 molar ratio), peaks start to disappear after 70h of calcination time, losing completely its crystalline structure after 100h at 380ºC. In dihydroxylation of kaolinite, Li_2CO_3 act as a "catalyst" activating this transformation. This result is evident in the thermal treatment at 550ºC for 30 min. While a complete amorphization happens in case of kaolin: Li_2CO_3 (1:1 molar ratio), kaolin requires longer calcination times at this temperature.

Fig.3showsrelative intensity of the X-ray diffraction peaks of kaolin and kaolin: Li_2CO_3 (1:1 molar ratio)with respect 20wt% of alumina standard, as a function of the square root of time for 380ºC, 470ºC, 550ºC temperatures. Relative intensities are calculated using the (001) diffraction peak of kaolinite (d=7.17424Å) taking that of corundum (113) as reference (d=2.08501Å). As it is shown in Fig. 3 a-c, the relative intensity for kaolin and kaolin: Li_2CO_3 (1:1 molar ratio) decreases as the temperature and time of calcination increases. Obtained values are always lower in kaolin: Li_2CO_3 (1:1 molar ratio) mixtures than in kaolinite. At 380ºC the relative intensity of kaolinite is very similar until 100h of calcination, afterwards this value decreases sharply. In the case of kaolin: Li_2CO_3 (1:1 molar ratio) mixture, the relative intensity decreases from the beginning and its value is close to zero after 100h of treatment. At 470ºC the difference in the relative intensity of kaolin and kaolin: Li_2CO_3 (1:1 molar ratio) is much more evident even at short calcination times, losing almost completely its crystalline structure after 16h of treatment. When the temperature is increased at 550ºC, relative intensity for kaolin: Li_2CO_3 (1:1 molar ratio) mixtures is very low, indicating that the presence of lithium anticipates the degradation of kaolinite.

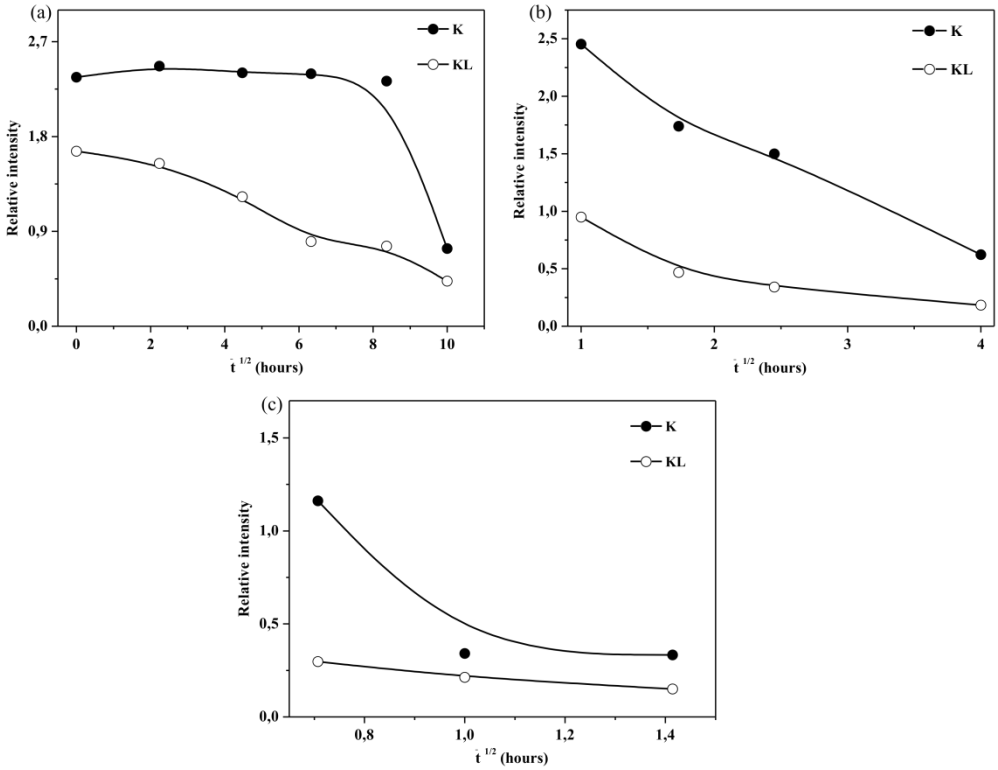

Figure 3. Variation of intensity vs square root of time for kaolin, K, (solid circle point) and kaolin: Li_2CO_3, KL, (1:1 molar ratio) (open circle point) at 380ºC (a), 470ºC (b) and 550ºC (c) of thermal treatment.

3.2. NMR spectroscopy

^{27}Al MAS-NMR spectra of kaolin and kaolin: Li_2CO_3 (1:1 molar ratio) treated powders are given in Fig.4a and b, respectively. ^{27}Al NMR spectra shows a single peak at 0 ppm which corresponds to the hexa-coordinated Al atom. After 70h at 380ºC only the 0ppm line can be observed in kaolin but a new peak at 60ppm associated with tetrahedral Al appears in kaolin: Li_2CO_3 mixtures. Increasing the calcination time of kaolin, ^{27}Al NMR spectra were composed of three lines located at 60, 30 and 0ppm assigned to Al in tetra-, penta- and hexacoordinated coordinations. According to the literature the component at 30ppm is rarely found in aluminosilicates [26]. In kaolin: Li_2CO_3 (1:1 molar ratio) powders, the increment of the 60ppm component goes parallel to the progressive dihydroxylation of the kaolinite. At 470ºC, the behavior is similar, but an increment of the temperature at 550ºC produces, after 30 minutes of treatment, a unique line at 0ppm in kaolin and two lines at 0 and 60ppm in the case of kaolin:Li_2CO_3 (1:1 molar ratio) mixtures.

From described results, it is clear that long treatments below 400ºC produce the amorphization of the kaolinite. In alkaline activated kaolin, samples showed tetrahedral Al (IV) with trace amounts of octahedral Al (VI) typical of geopolymers [27]. On the contrary, metakaolin contain Al (IV), Al (V) and Al (VI) species that transform in tetrahedral Al (IV) during alkaline activation. In resulting compounds, lithium ions must be associated with Al tetrahedra to maintain electronic neutrality of tetrahedral networks.

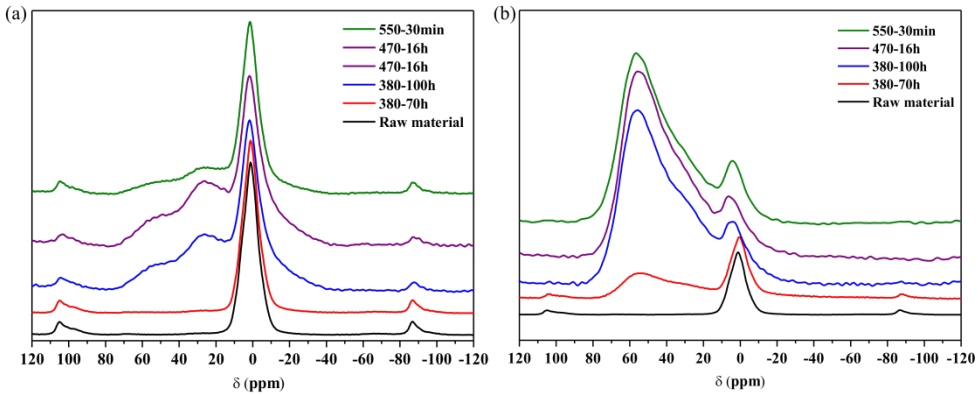

Figure 4. ^{27}Al MAS-NRM spectra for kaolin (a) and kaolin: Li_2CO_3 (1:1 molar ratio) (b)treated at different temperatures and times of calcination

^{29}Si NMR spectra of kaolin and kaolin: Li_2CO_3 (1:1 molar ratio) mixtures treated at different thermal treatments are given in Fig. 5a and b, respectively. In starting materials, a sharp absorption of ^{29}Si MAS NMR is observed at -91.5ppm that corresponds to Q^3 environments of the kaolinite. Increasing the temperature and time of calcination, this signal tends to disappear given rise to a broad component at -100ppm of the metakaolinite where tetrahedral sheets retain its initial arrangement. In this phase, the structural disorder increases producing an important broadening of the Si signal.

In the case of kaolin: Li_2CO_3 mixtures heated at 380ºC, the -91.5ppm component is also eliminated to give a broad component at -86ppm associated with the elimination of the kaolinite. This component was ascribed to Si tetrahedra, incorporated in amorphous more condensed networks than metakaolinite [13]. In the sample heated at 380ºC during 70h treatments, the intensity of the broad component increases at expenses of the narrow one. When sample is treated at 470 and 550ºC, the broad detected peak display similar characteristics to that of the sample heated at 380ºC/100h.

The position of the broad component differs in kaolin and kaolin: Li_2CO_3 (1:1 molar ratio) mixtures heated at similar temperatures, suggesting that the degree of Si condensation changes during reaction with Li_2CO_3 carbonates. In the first case, thermal treatment of the kaolin produces some dehydroxylation, however, in the second case, the broad line detected in ^{29}Si MAS-NMR spectrum must be ascribed to Si tetrahedra forming part of more condensed structures. In metakaolinite, the signal at -100ppm corresponds to lamellar structures (Q_3 environments) but in the alkaline activated kaolinite the signal detected has been associated with tri-dimensional (Q_4 environments) networks.

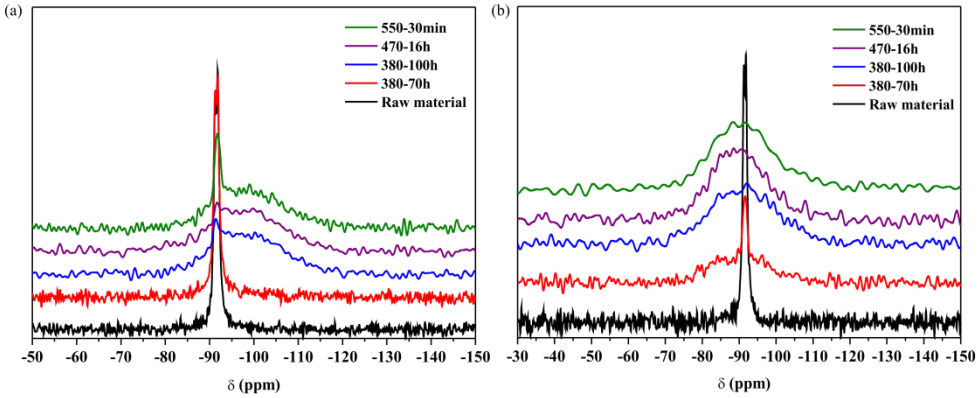

Figure 5. ^{29}Si MAS-NRM spectra of kaolin and kaolin: Li_2CO_3 (1:1 molar ratio) treated at different temperatures and times of calcination

^{7}Li MAS-NMR spectra of kaolin: Li_2CO_3 (1:1 molar ratio) treated at different temperatures and times of calcination are shown in Fig. 6. The ^{7}Li MAS-NMR spectra generally exhibit a broader signal at 0ppm, enlarged by dipolar and quadruple interactions. This component displays an intermediate Lorentzian/Gaussian character, indicating that Li ions display low mobility [28]. The ^{7}Li signal becomes narrower when the preparation temperature increases. Since both line shape and FWHM are controlled by lithium mobility, this result suggests that Li ions could become more mobile in calcined samples [28,29].

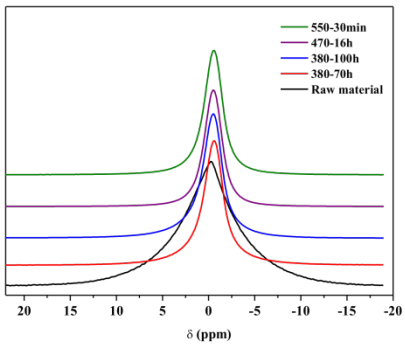

Figure 6. ^{7}Li MAS-NRM spectra of kaolin: Li_2CO_3 (1:1 molar ratio) treated at different temperatures and times of calcination

3.3. Spark Plasma Sintering

Amorphous kaolin: Li_2CO_3 (1:1 molar ratio) powder treated at 550ºC for 30min in air were sintered at 550ºC for 1h in air and at 550ºC for 5min under low and high vacuum in Spark Plasma Sintering equipment. The X-ray diffraction pattern of the sample calcined in air and in low vacuum (Fig. 7), shows that the material conserves the amorphous character of the starting material. However, when thermal treatment is performed in high vacuum the crystallization of the β-eucryptite was produced.

The formation of β-eucryptite ($LiAlSiO_4$) has been reported at temperatures near 800ºC [17,30], however in our case the crystallization of this phase was produced at a much lower temperature (500-550ºC). A possible explanation of this observation could be related with the sintering atmosphere used, since the presence of water and carbon dioxide in the atmosphere could promote the Li^+/H^+ exchange reaction and the formation of secondary phases at the surface of the particles that difficult the contact between contiguous grains [31].The presence of these moistures should be favored in sample sintered in air but decrease in low and high vacuum atmospheres.

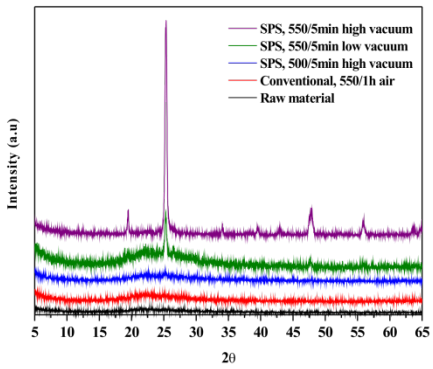

Figure 7. X-ray diffraction spectra for kaolin: Li_2CO_3 (1:1 molar ratio) raw material (black line), sintered at 550ºC in air (red line), 500ºC SPS in high vacuum (blue line), 550ºC SPS in low vacuum (green line) and 550ºC SPS in high vacuum (purple line)

3.4. XPS results

The X-ray photoelectron spectroscopy (XPS) was used to characterize the surface chemistry of samples. All samples were analyzed in the same conditions. Emission from O1s, C1s, Si2p, Al2p and Li1s core levels were detected with peak intensities depending on the sample preparation. In a second stage, the overall surface composition was estimated.

A detailed analysis of the Li1s emission corresponding to different samples is displayed in Fig.8. A single Li (1s) peak was observed at around 55.6eV that could be related to Li_2O [32]. Spectra were normalized to the maximum intensity detected values. A direct comparison of XPS spectra allowed the observation of subtle line shape differences. In-air treated sample, it was observed some broadening of the Li1s peak at the low binding energy side that has been ascribed to C-OH bonds.

Li ions should be allocated near Al tetrahedral to assure the charge-balance in the tetrahedral networks. This association does not eliminate chemical disorder. In these samples, the presence of different short range atomic arrangements lead to a wide distribution of atom environments or bonding configurations, producing an important broadening of the photoemission peak. This result is consistent with the amorphous nature of sample deduced from DRX patterns (see Fig. 7).

Once the sample is submitted to low vacuum conditions at 550ºC, a clear narrowing was detected that was associated with some crystallization detected in XRD patterns (Fig. 7). This effect is even more evident in

the case of the high vacuum SPS processing where the symmetry of Li1s peaks increases as a result of more uniform bonding configuration. This effect was not detected in Si2p and Al2p peaks which maintain the same line shape with independence of treatments.

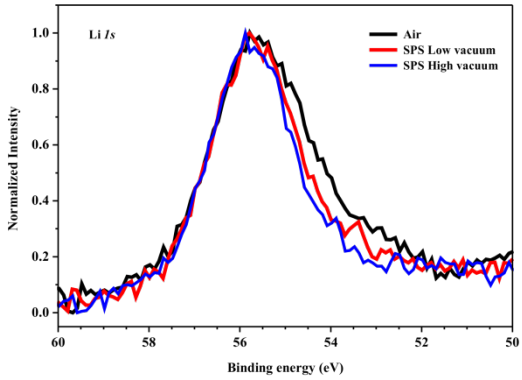

Figure 8. Normalized XPS spectra corresponding to Li1s core level emission from samples sintered at 550ºC in air (black line), SPS 550ºC in low vacuum (red line) and SPS 550ºC in high vacuum (blue line).

From the detailed analysis of C1s spectra recorded on different samples (see Fig. 9), it was observed that the carbon chemical environment is described by several components associated to C-C bonds with a binding energy of 284.5eV, C-O-H at 285.7 eV, O-C-O at 287.7eV and O-C=O at 289.5eV groups [33,34].In samples sintered at 550ºC in air and low vacuum C-OH links were detected. On the other hand, the presence of C=O links, was associated with the carbon diffusion from graphite molds used in SPS sintering, that are difficult to eliminate under low vacuum conditions. This result agrees with Li1s results showed in Fig. 8, where line is much narrower in the samples sintered in vacuum that in air. In the sample sintered with SPS at 550ºC under high vacuum it was observed that the amount of carbon associated with C-C links increases slightly compared with the sample sintered at low vacuum. In this sample the C-OH links disappeared and C-O and C=O links decreased because high vacuum helps its elimination.

Moreover, it is known that the atmosphere composition inside the SPS chamber affects the material's diffusivity during sintering [35]. The released gas, water, or organic compounds modify the thermodynamic driving force for the surface reduction and sintering. In particular, a high vacuum atmosphere cleaned the surface of the gains promoting the crystallization processes. Finally, low vacuum sintering increases the Li^+ bond inhomogeneity as a consequence of the OH^- and CO retention. In high vacuum sintered samples, inhomogeneity decrease and the elimination of adsorbed species facilitate the crystallization of β-eucryptite. In summary, XPS results agree with those deduced from X-ray diffraction in terms of local ordering and bonding environments.

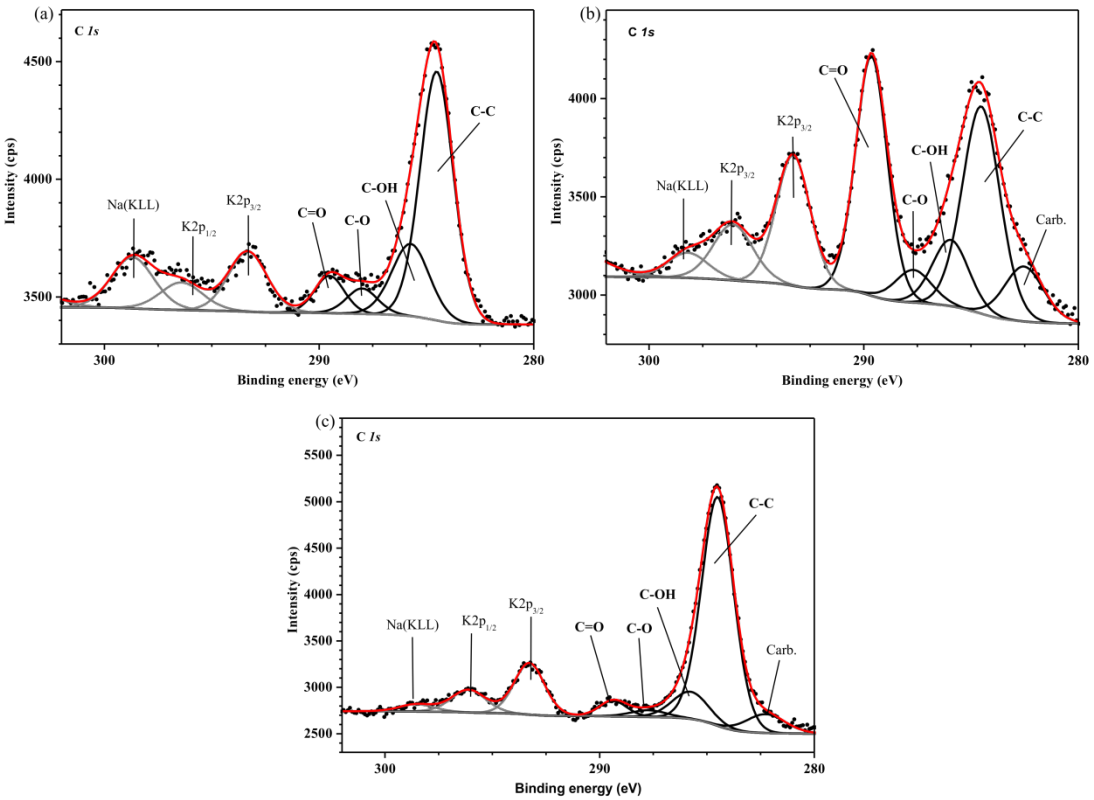

Figure 9. XPS spectra of carbon C1s from samples sintered at 550ºC in air (a), SPS 550ºC in low vacuum (b) and SPS 550ºC in high vacuum (c).

The density of the sintered samples was measured by Arquimedes method. The theoretical density used has been obtained by helium pycnometry. According to the results, sample sintered at 550ºC in air reaches only 54%th±0.5 since the presence of large pores hinders the complete densification of the material. The density of the samples sintered by Spark Plasma Sintering at 550ºC reaches values near 85%th±0.5 and 95%th±0.5 for low and high vacuum treatments. Two factors are involved in final density: 1) the pressure used during the SPS sintering that reduces the porosity and 2) the sintering atmosphere that favors the formation of β-eucryptite at low temperature.

3.5. NMR spectroscopy

Fig.10a-c show ^{27}Al, ^{29}Si and ^{7}Li MAS-NMR spectra of kaolin: Li_2CO_3 mixtures sintered in different conditions. In case of ^{27}Al spectra, the sample sintered at 550ºC in air showed similar spectra to starting powders before sintering. According to Fig.4b, peaks located near 0 and 60 ppm correspond to octa- and tetrahedral coordinated aluminium. Sample sintered at 550ºC in low vacuum show the same peaks, however, the intensity of the 0 ppm band is a bit lower suggesting an incipient crystallization of the β-eucryptite, in agreement with XRD results (Fig. 7). In the case of the sample sintered at 550ºC in high vacuum, only the tetrahedral Al peak of β-eucryptite was detected.

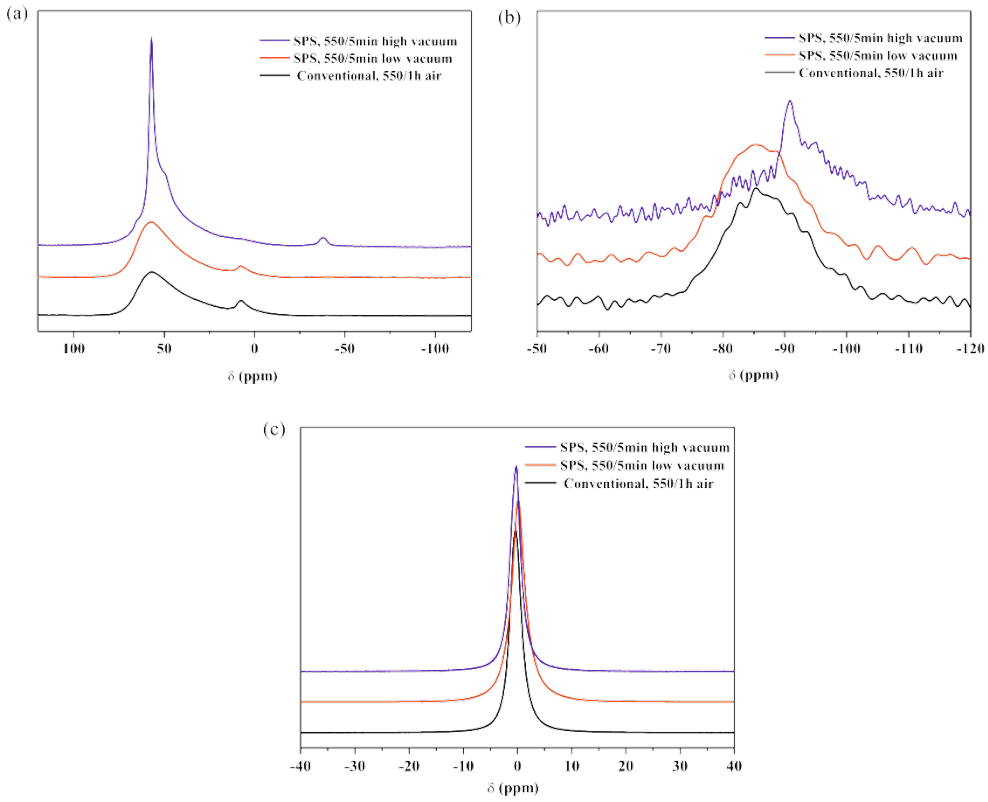

Figure 10.^{27}Al (a), ^{29}Si (b) and ^{7}Li (c) MAS-NRM spectra for kaolin: Li_2CO_3 (1:1 molar ratio) sintered in SPS at 550ºC in air (black line), 550ºC in low vacuum (red line) and 550ºC in high vacuum (blue line)

^{29}Si MAS-RMN spectra of samples depend on sintering conditions. Sample sintered at 550ºC in air and SPS in low vacuum shows a broad band between -75 and -100ppm, indicating that this specimen has not fully reacted [36], indicating the presence of a geopolymer with an amorphous structure. This band is displaced to more negative values at 550ºC with high vacuum. The peak detected near -91ppm corresponds to Si atoms of the β-eucryptite, surrounded by four Al in adjacent tetrahedra [37]. Described results suggest that alkaline activation of metakaolinite produce the liberation of silicate species that will be used in elaboration of more condensed structures. In new produced networks, Si and Al alternates in contiguous tetrahedra and Li atoms compensate charge deficits generated by Al incorporation. In polymerized networks, ^{7}Li MAS-NMR spectra display a signal centered at 0ppm. The full-width at half-maximum of the Li signal decrease progressively when Li coordination becomes better defined. The linewidth of components decrease considerably when β-eucryptite crystallites are produced.

3.6. FESEM

Scanning electron micrograph (SEM) of the fractured, polished and etched surface of samples sintered in air, low and high vacuum are present in Fig. 11a-c. The morphology of the polished samples before the etching treatment showed big pores in the sample sintered in air while a homogeneous microstructure with low porosity appeared in the samples sintered in SPS at low and high vacuum. A continuous phase is

observed in all samples but a large concentration of crystals with spherical shape, belonging to β-eucryptite was only obtained in SPS samples sintered at high vacuum treatments.

In general the response of phases toward acid attack can be classified into three different types: 1) very resistant, 2) low resistivity, and 3) decomposition of gelatinized phases. The etchant agent attacked regions of high residual stress and microcracked regions. It was assumed that the stability of the material depends basically on the type and concentration of crystalline phase, and composition and amount of residual glassy matrix [38]. After acid attack, part of the continuous phase is slightly dissolved being higher in samples with more amorphous phase due to their lower stability. High vacuum sintered samples display the lower dissolution compared with samples sintered in air and low vacuum atmospheres. According to the literature, lithium aluminosilicate phases like eucryptite, spodumene and β-quartz have excellent chemical stability toward acid attacks.

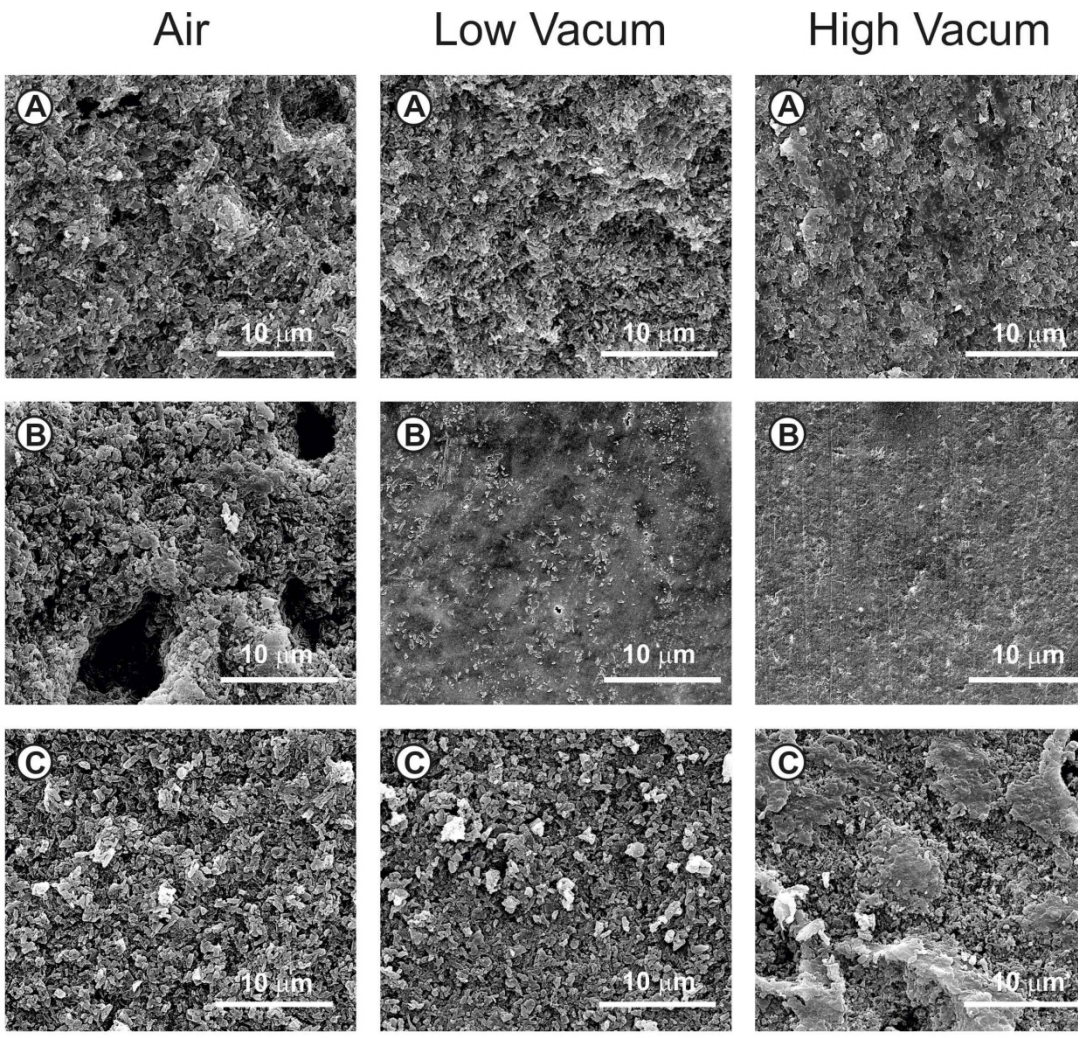

Figure 11. SEM micrographs of sintered samples in air and SPSed in low and high vacuum at 550ºC; (a) fractured surface, (b) polished surface and (c) etched surface.

Considering different detected fractures, the high vacuum sintered sample present a remarkable transgranular fracture while samples sintered in air and low vacuum display a type of intergranular fracture. According to the literature [39] intergranular fracture may indicate that ground boundaries are weaker than matrix grains.

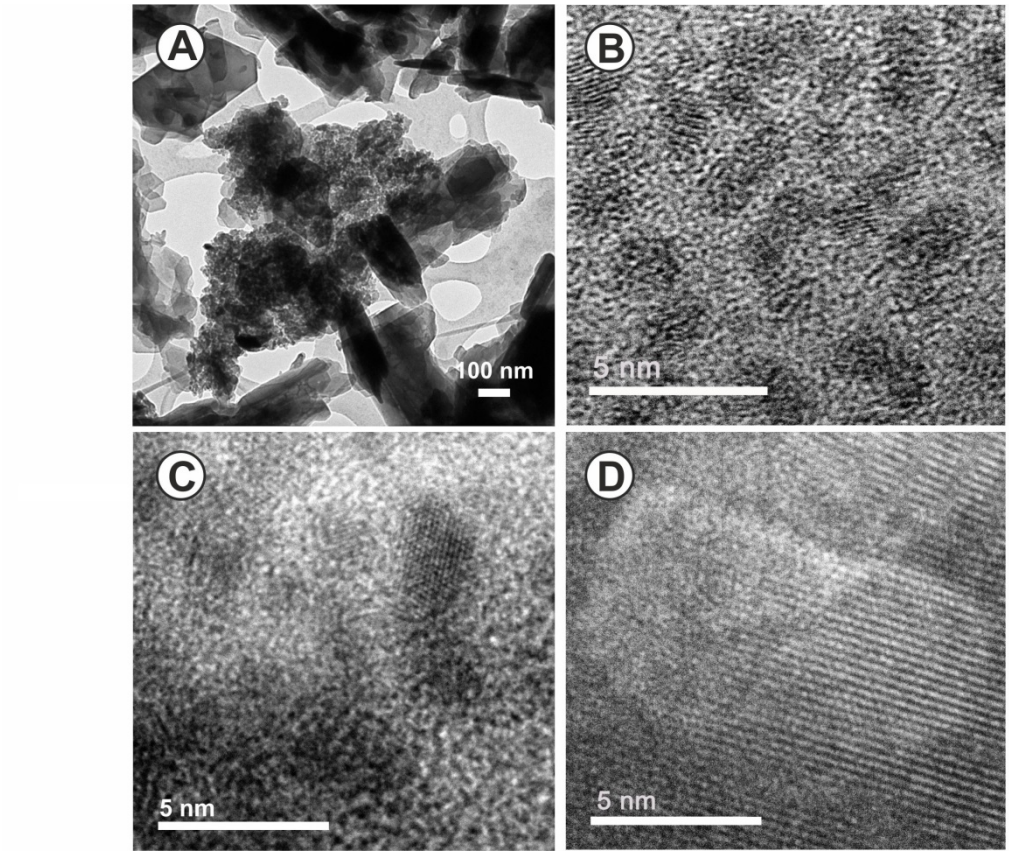

Figure 12.TEM micrographs corresponding to: (a) kaolin+Li_2CO_3 powder treated at 550ºC/30min in air; (b) SPS 500ºC vacuum; (c) SPS 550ºC low vacuum and (d) SPS 550ºC high vacuum

From the above results, it can be deduced that the formation of β-eucryptite from amorphous geopolymers depends on short-range diffusion within the amorphous geopolymer where both Si and Al are tetrahedraly coordinated. The lithium diffusion increased when the surface OH^- and C contents on amorphous geopolymer particles are eliminated in high vacuum SPS sintering treatments. This elimination induces the nucleation of a homogeneous distribution of nanocrystals as revealed in TEM micrographs (Fig. 12). At the low sintering temperature (500ºC-550ºC), the starting morphology of the geopolymer remains and Li ions migrate intoβ-eucryptite.

As indicated in TEM micrographics (Fig. 12), the crystallization proceeds by homogenous nucleation of 1-3nm β-eucryptite nano crystals at 500ºC in vacuum (not detected by XRD) (Fig. 12b). These nanocrystals growth to about 10nm at 550ºC (Fig. 12d), giving rise to new nanostructured β-eucryptite materials never reported in literature. The nanostructured β-eucryptite depicts the 3.51Å peak of $(\bar{1}12)$ reflection. Low vacuum atmosphere used in SPS sintering has a strong influence in crystallization and crystal size (5nm) of the β-eucryptite phase (Fig. 12c). This size was lower than in high vacuum 550ºC sintered samples.

In summary, alcaline activation of kaolinite favors the formation of amorphous geopolymer, where Si and Al are tetrahedrally coordinated in Q^4 environments. In the case of kaolinite activated with Na_2CO_3producedzeoliteprecursors but in the case of Li_2CO_3 activation β-eucriptite precursors are formed. From this fact, the study of different materials should be addressed: in the first case, compounds could be useful in Heterogeneous Catalysis [40, 41, 42], in the second case formed compounds could more adequate as solid electrolytes in batteries [43].

4. Conclusions

New material based on an amorphous Li-geopolymer has been synthesized by alkaline activation of kaolin with Li_2CO_3. The fabrication of both nanostructured β-eucryptite and amorphous Li-geopolymer compacts has been reported. The presence of lithium in the reactional medium anticipates the collapse of the kaolin network. It has been proven that the sintering atmosphere has also an important role in the lithium migration and crystallization of the material. For the first time, a dense (95%th) nanostructured (<10nm) β-eucryptite, $LiAlSiO_4$, compact is obtained by SPS at 550ºC in high vacuum. The results reported in the present investigation open new avenue of research on the possible exotic functional properties, i.e. null thermal expansion, ionic conduction, as well as mechanical properties of both β-eucryptite nanostructured and amorphous compacts. In the future, the SPS processing of ceramics under different atmospheres will be extended to the preparation of novel materials with outstanding properties.

Acknowledgements

The authors acknowledge the Principado de Asturias for funding through the projects GRUPIN IDI/2018/000232 and MAT2016-78362-C4-2.

A. Borrell acknowledges the Spanish Ministry of Economy and Competitiveness for her RyC contract (RYC-2016-20915).

[1]M. DamilolaOlawale. Syntheses, Characterization and binding strength of geopolymers: A review, Int. J. Mater. Sci. and applications 2 (2013) 185-193.

[2]H. Zain, M. Mustafa Al Bakri Abdullah, K. Hussin, N. Ariffin, R. Bayuaji, Review on various types of geopolymer materials with the environmental impact assessment. Matec Web of Conferences, 97 (2017) 01021

[3]H. Xu, J. S. J. Van Deventer. The geopolymerisation of alumino-silicate minerals, Int. J. Miner.Process. 59 (2000) 247-266.

[4]S. Hanjitsuwan, P. Chindaprasirt, K. Pimraksa, Electrical conductivity and dielectric properties of fly ash geopolymerpastes, Int. J. Miner. Metall. Mater. 18(2011) 94

[5]K. Komnitsas, D. Zaharaki, Utilisation of low-calcium slags to improve the strength and durability of geopolymers.Geopolymers - Structure,processing, properties and industrial applications. Woodhead Publishing Limited, Oxford,Cambridge, New Delhi, 2009, pp. 343-375.

[6]F. Pacheco-Torgal, S. Jalali, J.P. Castro-Gomes, Utilization of mining waste to producegeopolymer binders, in: J.L. Provis, J.S.J. van Deventer (Eds.) Geopolymers - Structure,processing, properties and industrial applications Woodhead Publishing Limited, Oxford,Cambridge, New Delhi, 2009, pp. 267-293.

[7]D. D. BurduhosNergis, M. M. A. B. Abdullah, P. Vizureanu, M. F. M. Tahir. Geopolymers and their uses: Review. IOP Conf. Series: Materials Science and Engineering 374 (2018) 012019

[8]A. Autef, E. Joussein, A. Poulesquen, G. Gasgnier, S. Pronier, I. Sobrados, J. Sanz, S. Rossignol, Influence of metakaolin purities on potassium geopolymerformulation:The existence of several networks, J. Colloid Interface Sci. 408 (2013) 43–53.

[9]M. B. Ramli, A.O. Richard, Characterization of metakaolin and study on early age mechanical strength of hybrid cementitiouscomposites.Construction and building materials 121 (2016) 599-611.

[10] F. Zhang, L. Zhang, M. Liu, Ch. Mu, Y. Nan Liang, X. Hu, Role of alkali cation in compressive strength of metakaolin based geopolymers,Ceram. Int. 43 (2017) 3811-3817.

[11]M. Luz Granizo, M. T. Blanco-Varela, S. Martínez-Ramírez, Alkali activation of metakaolin: parameters affecting mechanical, structural and microstructural properties,J. Mater. Sci. 42 (2007) 2934-2943.

[12]M. L. Granizo, M. T. Blanco-Varela, A. Palomo. Influence of the starting kaolin on alkali-activated materials based on metakaolin. Study of the reaction parameters by isothermal conduction calorimetry. Journal of Materials Science 35 (2000) 6309-6315.

[13]A. Madani, A. Aznar, J. Sanz, J. M. Serratosa, ^{29}Si and ^{27}Al NMR study of zeolite formation from alkali-leached kaolinite. Influence of thermal preactivation, Phys. Chem. 94 (1990) 760-765

[14]S. J. O´Connor, K. J. D. MacKenzie, Synthesis, characterization and thermal behavior of lithium aluminosilicate inorganic polymers, J. Mater. Sci. 45 (2010)3707-3713.

[15]A. GarcíaVerduch, J. S. Moya Corral, Reaction at low temperatures between kaolin and lithium carbonate, International ClayConference (1972).

[16]O. García-Moreno, A. Fernández, R. Torrecillas, Conventional sintering of LAS-SiCnanocomposites with very low thermal expansion coefficient, J. Eur. Ceram. Soc. 30 (2010) 3219-3225

[17]O. García-Moreno, A. Fernández, R. Torrecillas,Solid state sintering of very low and negative thermal expansion ceramics by Spark Plasma Sintering, Ceram. Int. 37 (2011) 1079-1083

[18]O. García-Moreno, A. Fernández, R. Torrecillas,Sintering of mullite-β-eucryptite ceramics with very low thermal expansion, Int. J. Mat. Res. 103 (2012) 4

[19] O. García-Moreno, A. Borrell, B. Bittmann, A. Fernández, R. Torrecillas, Alumina reinforced eucryptite ceramics: very low thermal expansion material with improved mechanical properties, J. Eur. Ceram. Soc. 31 (2011) 1641-1648

[20] R. Benavente, M. D. Salvador, O. García-Moreno, F. L. Peñaranda-Foix, J. M. Catalá-Civera, A. Borrell. Microwave, spark plasma and conventional sintering to obtain controlled-thermal-expansion β-eucryptite materials, Ceram. Int. 40 (2014) 935-941.

[21]Nazneen, S. C. Daggubati, V. Lakshminarayana. Geopolymer- a potential alternative binder for the sustainable development of concrete without ordinary Portland cement. Jr. of Industrial Pollution Control 33 (S3) (2017) 1500-1504.

[22]R. T. Johnson Jr, B. Morosin, M. L. Knotek, R.M. Biefeld. Ion conductivity in $LiAlSiO_4$. Physics letters 54A 5 (1975) 403-404

[23]Y. Chen, S. Manna, C. V. Ciobanu, I. E. Reimanis, Thermal regimes of Li-ion conductivity in β-eucryptite, J. Am. Ceram. Soc. 101 (2017) 1-9

[24]A. M. Rashad,Metakaolin as cementitious material: History, scours, production and composition-A Comprehensive overview, Construction and building materials 41 (2013) 303-318.

[25] E. Erasmus, The influence of thermal treatment on properties of kaolin, Hem. Ind. 70 (2016) 595-601.

[26] J. Sanz, A. Madani, J. M. Serratosa, J. S. Moya, S. Aza, Aluminum-27 and Silicon-29 Magic- Angle Spinning Nuclear Magnetic Resonance Study of the Kaolinite-MulliteTransformation, J. Am. Ceram. Soc. 71 (1988) C-418-C-421

[27] P. Duxson, A. Fernández-Jiménez, J. L. Provis, G.C. Lukey, A. Palomo, J. S. J. van Deventer,Geopolymer technology: the current state of the art, J. Mater.Sci. 42 (2007) 2917-2933

[28] L. Barbieri, C.Leonelli, T.Manfredini, C.Siligardi, A. BonamartiniCorradi, Nucleation and Crystallization of a Lithium Aluminosilicate Glass, J. Am. Ceram. Soc. 80 (1997) 3077-83

[29] A. Castillo, T.Charpentier, O.Rapaud, N.Pradeilles, S.Yagoubi, E. Foy, M. Moskura, H. Khodja, Bulk Li mobility enhancement in Spark Plasma Sintered Li(7-3x)AlxLa3Zr2O12 garnet, Ceram. Int. 44 (2018) 18844-18850

[30] S. J. O´Connor, K. J. D. Mackenzie, Synthesis, characterization and thermal behavior of lithium aluminosilitate inorganic polymers, J. Mater Sci. 45 (2010)3707-3713

[31]F. Aguesse, J. Miguel López del Amo, B.Roddatis, A.Aguadero, J. A. Kilner,Enhancement of the grain boundary conductivity in ceramic Li0.24La0.55TiO3 electrolytes in a moisture –free processing environment, Adv. Mater.Inter. 1 (2014) 1300143.

[32] K. N. Wood, G. Teeter. XPS on Li-battery-related compounds: Analysis of inorganic SEI phases and a methodology for charge correction, Appl. Energy Mater. 1 (2018) 4493-4504.

[33]T.Grzybek, K.Kreiner, Surface changes in coals after oxidation. 1. X-ray photoelectron spectroscopy studies, Langmuir 13(1997) 909-912.

[34] S. R. Kelemen, M. Afeworki, M. L. Gorbaty, Characterization of organically bound oxygen forms in lignites, peats and pyrolyzed peats by x-ray photoelectron spectroscopy (XPS) and solid-state 13C NMR methods,Energy&Fuels16 (2002) 1450-1462.

[35]G. Franceschin, N. Flores-Martínez, G. Vázquez-Victorio, S. Ammar, R. Valenzuela,Sintering and reactive sintering by spark plasma sintering (SPS), Chapter 6, Intechopen.

[36]P.Duxson, J. L. Provis, G. C. Lukey, F.Separovic, J. S. J. van Deventer, 29Si NMR study of structural ordering of aluminosilicategeopolymergels, Langmuir 21 (2005) 3028-3036

[37] B. L. Phillips, H. Xu, P. J. Heaney, A. Navrotsky, 29Si and 27Al MAS-NMR spectroscopy of β-eucryptite (LiAlSiO4): The enthalpy of Si, Al ordering, Amer.Mineral. 85 (2000) 181-188

[38]S. M. Salman, S. N. Salama, H. A. Abo-Mosallam, Crystallization characteristics and phisico-chemical properties of glass-ceramic based on Li2O-ZnO-SiO2 system, Bol. Soc.Esp. Ceram.Vidr. 56 (2017) 205-214.

[39]G. D. Quinn, Fractography of ceramics and glasses, Practice guide, National Institute of Standards and Technology.

[40] M. I. M. Al-Zeer, K. J. D. MacKenzie, Fly ash-based geopolymers as sustainable bifunctional heterogeneous catalyst and their reactivity in friedel-crafts acylation reactions, Catalysts 9 (2019) 372.

[41] M. D. M. Innocentini, R. F. Botti, P. M. Bassi, C. F. P. R. Paschoalato, D. L. Flumignan, G. Franchin, P. Colombo. Lattice-shaped geopolymer catalyst for biodiesel synthesis fabricated by additive manufacturing, Ceram. Int. 45 (2019) 1443-1446.

[42] P. Sazama, O. Bortnovsky, J. Dědeček, Z. Tvarůžková, Z. Sobalík, Geopolymer based catalysts- new group of catalytic materials, Catalysis Today 164 (2011) 92-99.

[43]R. T. Johnson, B. Morosin, M. L. Knotek, R. M. Biefeld, Ionic conductivity in $LiAlSiO_4$, Phys. Lett. 54A (1975) 403-404.